Supplementary Materials

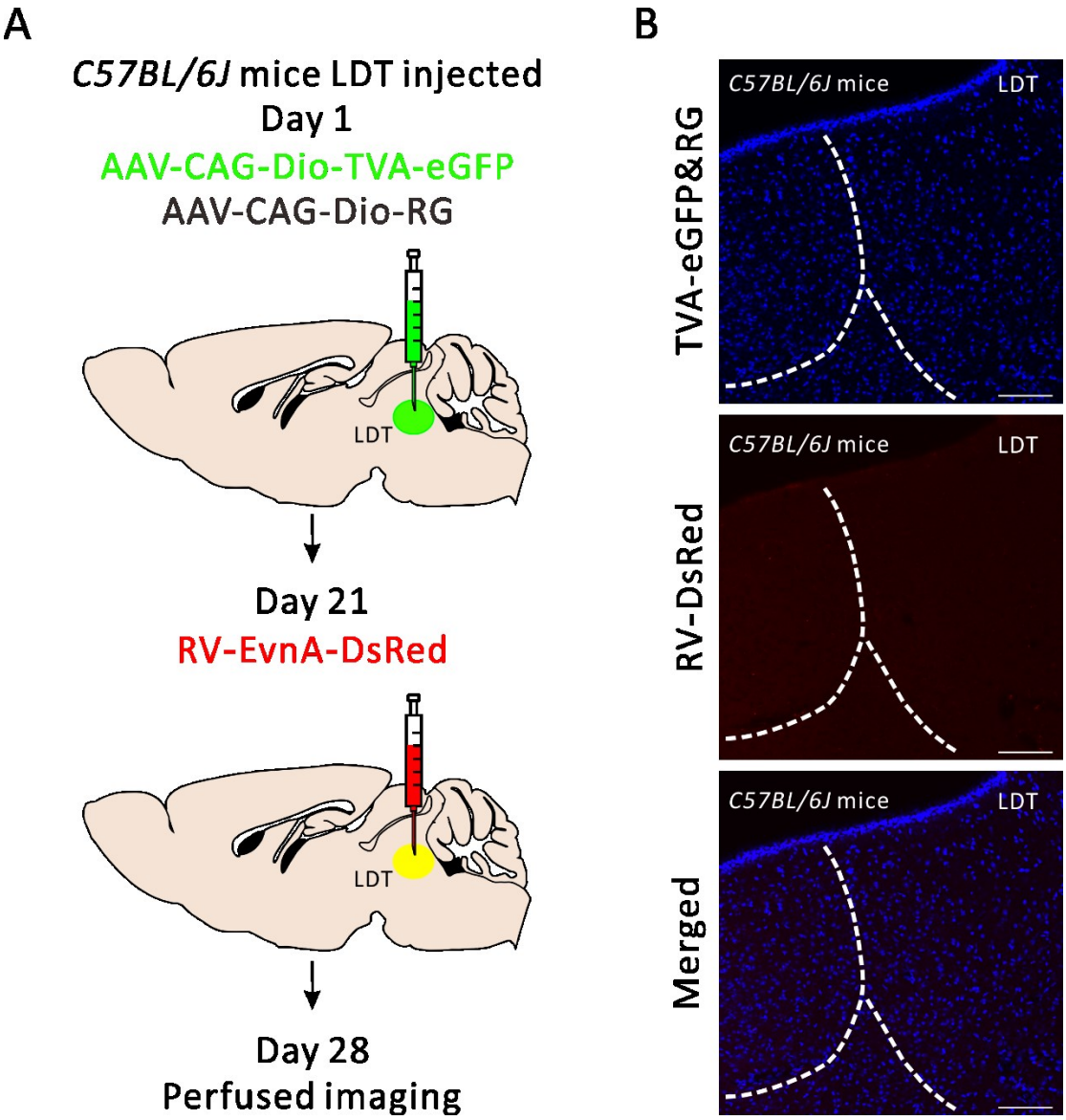

Supplementary Figure 1, Control experiment demonstrating specificity of retrograde trans-synaptic tracing approach.

A, Timeline of virus injection into the LDT of wild-type mice for retrograde trans-synaptic tracing. The experiment is related to Figure 1 A.

B, Representative confocal images of LDT neurons in wild-type mice. No evidence of TVA-eGFP or RV-DsRed fluorescence positive cells was observed.

Abbreviations

AI	agranular insular cortex
BST	bed nucleus of the stria terminalis
Ce	central amygdaloid nucleus
CG	central gray
Cg	cingulate cortex
CIC	central nucleus of the inferior colliculus
CnF	cuneiform nucleus
DMTg	dorsomedial tegmental area
DR	dorsal raphe nucleus
DTg	dorsal tegmental nucleus
DpMe	deep mesencephalic nucleus
IP	interpeduncular nucleus
LHb	lateral habenular nucleus
LH	lateral hypothalamic area
LO	lateral orbital cortex
LPAG	lateral periaqueductal gray
LPB	lateral parabrachial nucleus
LDT	laterodorsal tegmental nucleus
M	motor cortex
MnR	median raphe nucleus
MO	medial orbital cortex
MPA	medial preoptic area
PAG	periaqueductal gray
PH	posterior hypothalamic area
PnC	pontine reticular nucleus, caudal part
PnO	pontine reticular nucleus, oral part
PrL	prelimbic cortex
PtA	parietal association cortex
PPTg	pedunculopontine tegmental nucleus
RS	retrosplenial cortex
S	somatosensory cortex
SC	superior colliculus
SN	substantia nigra
VLPAG	ventrolateral periaqueductal gray
VO	ventral orbital cortex
VTA	ventral tegmental area
ZI	zona incerta

Supplementary Figure 2, List of structures in Figure 2 to Figure 8.

A

	VGLUT2-Cre	CHAT-Cre	PV-Cre	SST-cre
AcbSh	√		√	√
AHP	√	√	√	√
APT	√	√		
CPU	√	√	√	
DLPAG	√	√	√	√
DM	√	√	√	√
Eth				√
IL	√			
LC	√	√	√	√
LM	√		√	√
LPO	√	√		√
MM	√	√		
MPO	√	√	√	√
PF	√	√	√	√
PVA			√	
PoT	√			
VDB	√	√	√	√
VMH	√	√	√	√
VP	√	√	√	√

B

Abbreviations

AcbSh	accumbens nucleus, shell
AHP	anterior hypothalamic area, posterior part
APT	anterior pretectal nucleus
CPU	catudate putamen
DLPAG	dorsolateral periaqueductal gray
DM	dorsomedial hypothalamic nucleus
Eth	ethmoid thalamic nucleus
IL	infralimbic cortex
LC	locus coeruleus
LM	lateral mammillary nucleus
LPO	lateral preoptic area
MM	medial mammillary nucleus, medial part
MPO	medial preoptic nucleus
PF	parafascicular thalamic nucleus
PVA	paraventricular thalamic nucleus, anterior part
PoT	posterior thalamic nuclear group, triangular part
VDB	nucleus of the vertical limb of the diagonal band
VMH	ventromedial hypothalamic nucleus
VP	ventral pallidum

Supplementary Figure 3, List of brain areas or subareas which accounted for <1% of total inputs.

Data	Statistical test	p value	Multiple comparisons		
Figure 1C	One-way ANOVA	0.5299	—		
Figure 6A					
Cortex	One-way ANOVA	0.006	Turkey's multiple comparisons test :	VGLUT2-Cre vs CHAT-Cre	p=0.016
				VGLUT2-Cre vs PV-Cre	p=0.007
				VGLUT2-Cre vs SST-Cre	p=0.029
				CHAT-Cre vs PV-Cre	p=0.955
				CHAT-Cre vs SST-Cre	p=0.986
				PV-Cre vs SST-Cre	p=0.831
Thalamic	Kruskal-Wallis test	0.0386	Dunn's multiple comparisons test :	VGLUT2-Cre vs CHAT-Cre	adj. p=0.1051
				VGLUT2-Cre vs PV-Cre	adj. p=0.1879
				VGLUT2-Cre vs SST-Cre	adj. p>0.9999
				CHAT-Cre vs PV-Cre	adj. p>0.9999
				CHAT-Cre vs SST-Cre	adj. p=0.7137
				PV-Cre vs SST-Cre	adj. p>0.9999
Hypothalamic	One-way ANOVA	<0.0001	Turkey's multiple comparisons test :	VGLUT2-Cre vs CHAT-Cre	p<0.0001
				VGLUT2-Cre vs PV-Cre	p<0.0001
				VGLUT2-Cre vs SST-Cre	p=0.088
				CHAT-Cre vs PV-Cre	p=0.927
				CHAT-Cre vs SST-Cre	p=0.012
				PV-Cre vs SST-Cre	p=0.04
Midbrain	One-way ANOVA	0.395	—		
Hindbrain	One-way ANOVA	0.023	Turkey's multiple comparisons test :	VGLUT2-Cre vs CHAT-Cre	p=0.283
				VGLUT2-Cre vs PV-Cre	p=0.014
				VGLUT2-Cre vs SST-Cre	p=0.309
				CHAT-Cre vs PV-Cre	p=0.309
				CHAT-Cre vs SST-Cre	p>0.9999
				PV-Cre vs SST-Cre	p=0.283
Figure 7A					
M	One-way ANOVA	0.027	Turkey's multiple comparisons test :	VGLUT2-Cre vs CHAT-Cre	p=0.055
				VGLUT2-Cre vs PV-Cre	p=0.029
				VGLUT2-Cre vs SST-Cre	p=0.349
				CHAT-Cre vs PV-Cre	p=0.983
				CHAT-Cre vs SST-Cre	p=0.649
				PV-Cre vs SST-Cre	p=0.443
PrL	Kruskal-Wallis test	0.0786	—		
VO	Kruskal-Wallis test	0.0003	Dunn's multiple comparisons test :	VGLUT2-Cre vs CHAT-Cre	adj. p=0.0082
				VGLUT2-Cre vs PV-Cre	adj. p=0.2663
				VGLUT2-Cre vs SST-Cre	adj. p>0.9999
				CHAT-Cre vs PV-Cre	adj. p>0.9999
				CHAT-Cre vs SST-Cre	adj. p=0.0841
				PV-Cre vs SST-Cre	adj. p>0.9999
Cg	Kruskal-Wallis test	0.0169	Dunn's multiple comparisons test :	VGLUT2-Cre vs CHAT-Cre	adj. p=0.0288
				VGLUT2-Cre vs PV-Cre	adj. p=0.7137
				VGLUT2-Cre vs SST-Cre	adj. p=0.1879
				CHAT-Cre vs PV-Cre	adj. p>0.9999
				CHAT-Cre vs SST-Cre	adj. p>0.9999
				PV-Cre vs SST-Cre	adj. p>0.9999
S	One-way ANOVA	0.093	—		
RS	One-way ANOVA	0.584	—		
LO	One-way ANOVA	0.066	—		
PtA	Kruskal-Wallis test	0.1309	—		
MO	Kruskal-Wallis test	0.0215	Dunn's multiple comparisons test :	VGLUT2-Cre vs PV-Cre	adj. p=0.0423
				VGLUT2-Cre vs SST-Cre	adj. p>0.9999
				PV-Cre vs SST-Cre	adj. p=0.1485
AI	Kruskal-Wallis test	0.0173	Dunn's multiple comparisons test :	VGLUT2-Cre vs PV-Cre	adj. p=0.0418
				VGLUT2-Cre vs SST-Cre	adj. p=0.0734
				PV-Cre vs SST-Cre	adj. p>0.9999
Figure 8C	Kruskal-Wallis test	0.0024	Dunn's multiple comparisons test :	VGLUT2-Cre vs CHAT-Cre	adj. p=0.3806
				VGLUT2-Cre vs PV-Cre	adj. p=0.0085
				VGLUT2-Cre vs SST-Cre	adj. p>0.9999
				CHAT-Cre vs PV-Cre	adj. p>0.9999
				CHAT-Cre vs SST-Cre	adj. p>0.9999
				PV-Cre vs SST-Cre	adj. p=0.2701
Figure 8D	One-way ANOVA	0.092	—		

Supplementary Table 1, Details of the statistical analysis.